Effect of solvents on the intercalation/de-intercalation behaviour of monovalent ionic species from non-aqueous solvents on polypropylene–graphite composite electrode

R. Santhanam, M. Noel *

Central Electrochemical Research Institute, Karaikudi-630 006, India

Abstract

The intercalation/de-intercalation efficiency (IDE) of monovalent cationic (Li^+, Na^+, K^+ and TBA^+) and anionic (ClO_4^-, BF_4^-) species in different non- aqueous solvents are compared under otherwise identical experimental conditions using cyclic voltammetry, X-ray diffraction (XRD), thermogravimetry (TG) and differential thermal analysis (DTA). Dimethyl sulfoxide (DMSO), dimethylformamide (DMF) and propylene carbonate (PC) are found to be the solvents of choice for cationic intercalation. PC and acetonitrile (AN) are found to be the solvents of choice for anionic intercalation. Among the cations strongly solvated Li^+ shows better IDE when compared with Na^+ and K^+. TBA^+ appears to undergo efficient intercalation without a solvation sheath. The effect of concentration and intercalation potential on the overall IDE is also reported. A new intercalated phase is confirmed by XRD, TG and DTA.

Keywords: Graphite electrodes; Intercalation; Non-aqueous solvents

1. Introduction

The electrochemical intercalation of monovalent cations such as lithium (Li^+), sodium (Na^+), potassium (K^+) and tetrabutyl ammonium (TBA^+) ions on graphite electrodes from non-aqueous solvents such as dimethyl sulfoxide (DMSO), dimethoxyethane (DME) and propylene carbonate (PC) was reported as early as 1975 [1,2]. Severe disintegration of graphite is noticed when fairly large cationic species such as tetraoctyl ammonium cations are employed [3]. With the recent interest in lithium-ion intercalated battery systems, this process has evoked renewed study. Intercalation/de-intercalation processes on carbon fibres [4], thermal changes during intercalation/de-intercalation processes [5], and graphite lattice transformations [6] in non-aqueous solvents are some of the investigations reported recently. It is generally agreed that solvated cationic species are involved in the intercalation process. A recent study suggests, however, the possibility of desolvated lithium-ion intercalation [7]. Crown ethers suppress solvent decomposition and thus enhance intercalation/de-intercalation efficiency (IDE) [8]. Extensive studies on the chemistry of graphite [9,10] and carbon fibres [10] on lithium-interca-

lated electrodes in connection with battery applications have been reported. The intercalation/de-intercalation processes are shown [11] to proceed predominantly through the edge planes. Though cationic intercalation studies are mainly confined to monovalent cations, Maeda and co-workers [12,13] have recently reported efficient intercalation of divalent cations like Mg^{2+} and Mn^{2+} from DMSO. There have also been reports of quite efficient intercalation of perchlorate (ClO_4^-) [14,15] and fluoborate (BF_4^-) [8] anions on graphite fibre [14,15] and graphite sheet [15] from propylene carbonate (PC) medium. In both cases, intercalation is an exothermic process and de-intercalation is an endothermic one.

The possibility of utilizing tetrabutyl ammonium perchlorate (TBAP) in a PC medium as a dual-intercalation battery system (cation-intercalated system as anode, and anion-intercalated system as cathode) has been briefly outlined in a recent study from this laboratory [16]. Though cationic as well as anionic intercalation/de-intercalation processes have been reported from different non-aqueous solvents by different workers [1–15], no direct comparison of all these ionic species in different solvents under otherwise identical experimental conditions is available in the literature. This is the primary objective of this work. Generally, intercalation and de-intercalation studies have been confined to carbon fibre or graphite electrodes. A polypropylene–graphite composite

---

* Corresponding author.

electrode was employed earlier by Beck and co-workers [17–19] for anionic intercalation studies from aqueous acidic media. This electrode exhibited better stability as well as reproducibility in non-aqueous solvents [16,20] and hence, was chosen for the present study.

2. Experimental

A polypropylene–graphite composite (CPP) electrode was used throughout the study as the working electrode.

A rod of 3 mm diameter, machined from the CPP sample mentioned above, was tight-fitted into Teflon and used as the working electrode. The electrode was polished using emery papers (1/0 to 5/0) and the reversibility was checked with a ferricyanide/ferrocyanide redox system ($\Delta E_p < 65$ mV). A saturated calomel electrode and a platinum electrode were used as the reference and counter electrodes, respectively.

Analar grade and distilled non-aqueous solvents, DMSO [21], DMF [22] and PC [23] were used throughout the work.

The X-ray diffraction (XRD) studies were carried out using a JEOL (Model JDX-3080) computer-controlled X-ray diffractometer. Thermogravity (TG) and differential thermal analysis (DTA) were carried out in a computer-controlled thermal analyser (Model STA 1500, PL Thermal Sciences, UK).

All other experimental details are described elsewhere [16,20,24].

3. Results and discussion

3.1. Effect of solvent

3.1.1. Cationic intercalation

The intercalation/de-intercalation behaviour of monovalent cationic species was indeed found to depend significantly on the nature of the solvent for each cationic species. Typical
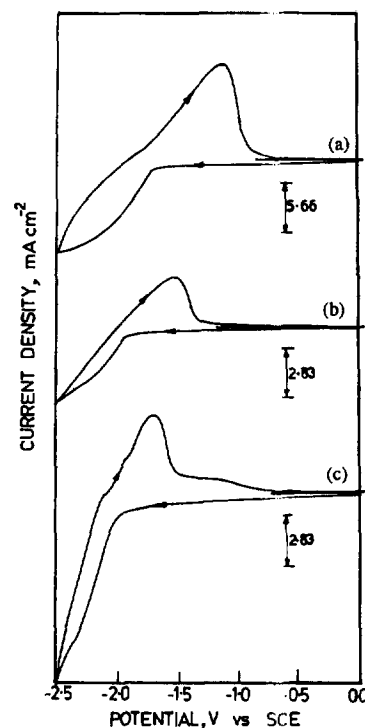

Fig. 1. Cyclic voltammogram for the reductive intercalation of CPP electrode in (a) DMSO, (b) PC and (c) DMF containing 0.25 M LiClO$_4$; scan rate = 40 mV s^{-1}.

cyclic voltammetric responses showing reductive intercalation and oxidative de-intercalation peaks for 0.25 M lithium perchlorate (LiClO$_4$) in DMSO, PC and DMF are presented in Fig. 1(a)–(c), respectively. Lithium ions show good intercalation/de-intercalation behaviour in all three solvents. Some qualitative differences with respect to the sharpness of intercalation as well as de-intercalation responses may be noticed. The intercalation charge (Q_{in}), the de-intercalation charge (Q_{di}), the intercalation/de-intercalation efficiency (Q_{di}/Q_{in} or IDE), the threshold potential for the beginning of intercalation (E_{th}) and the de-intercalation peak potential (DPP) obtained from these cyclic voltammograms are summarised in Table 1 for all three solvents. For lithium ions, the

Table 1
Cyclic voltammetry data for cationic intercalation/de-intercalation processes on a CPP electrode: solvent effects; concentration = 0.25 M; scan rate = 40 mV s^{-1}

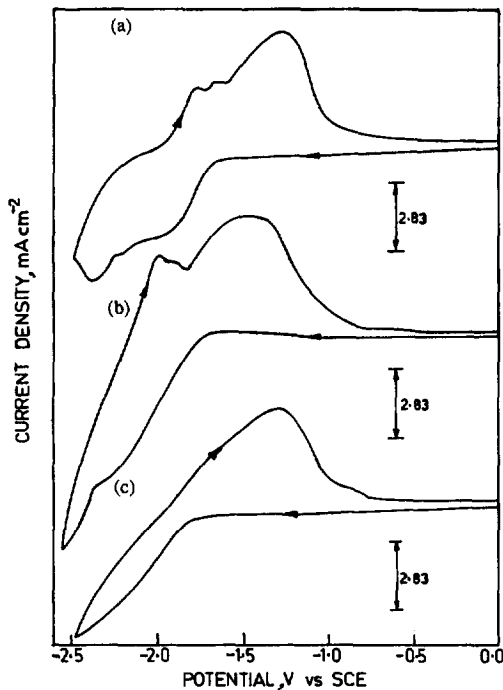| Ion	Solvent	DPP (V)	E_{th} (V)	Q_{in} (mC/cm^2)	Q_{di} (mC/cm^2)	Q_{di}/Q_{in} (or IDE)
Li$^+$	DMSO	−1.14	−1.70	169.68	102.52	0.60
	PC	−1.54	−1.92	57.46	24.68	0.43
	DMF	−1.70	−1.94	99.05	37.07	0.38
Na$^+$	DMSO	−0.96	−1.72	337.25	236.85	0.70
	PC					
	DMF					
K$^+$	DMSO	−1.08	−1.72	431.27	234.23	0.54
	PC					
	DMF					
TBA$^+$	DMSO	−1.26	−1.62	99.41	73.32	0.74
	PC	−1.40	−1.72	112.80	68.40	0.61
	DMF	−1.30	−1.82	80.95	40.13	0.50

Fig. 2. Cyclic voltammogram for the reductive intercalation of CPP electrode in (a) DMSO, (b) DMF and (c) PC containing 0.25 M TBAP; scan rate = 40 mV s^{-1}.

IDE is found to be always greater than 0.38 and the best IDE value of 0.60 is obtained in DMSO.

Quite different solvent effects are noticed for Na$^+$ and K$^+$ ions. For both these cations, a good IDE is noticed only in DMSO (Table 1). In the other two solvents the de-intercalation peak is totally absent. In DMSO, however, the IDE is fairly high for both Na$^+$ (0.70) and K$^+$ (0.54). The intercalation/de-intercalation behaviour of TBA$^+$ cations once again is found to be quite efficient in all three solvents (Fig. 2). Fairly high Q_{in} and Q_{di}, as well as a high IDE, are found in DMSO (Fig. 2(a)), DMF (Fig. 2(b)) and PC (Fig. 2(c)). Three distinct intercalation peaks and corresponding de-intercalation peaks are specifically noticed in DMSO. The IDE also shows the maximum value of 0.74 in this medium (Table 1).

At first sight, the dependence of solvent on the intercalation of all these four cations under otherwise identical conditions (summarized in Table 1) appears somewhat perplexing. Earlier works have also reported efficient Na$^+$ and K$^+$ intercalation only in DMSO [1,2,12,13]. Li$^+$ cations and tetraalkyl ammonium cations, however, are also found to undergo efficient intercalation/de-intercalation in other solvents [1–3]. To date, no distinct explanation for this solvent dependence of monovalent cationic intercalation has been advanced.

The following explanation may be offered for this observation. Graphite is in a relatively hydrophobic environment, especially under cathodic polarization conditions where graphite oxidation will be negligible. The intercalated species also would require a non-polar or hydrophobic environment for efficient intercalation. The TBA$^+$ cation does not require a solvation sheath for efficient intercalation as it is essentially surrounded by hydrocarbon chains. For Li$^+$, Na$^+$ and K$^+$ ions, however, the intercalation would be efficient only when they are strongly solvated. Li$^+$ ions are inherently strongly solvating in character and, hence, they can form solvated species with all the solvents and intercalation/de-intercalation would be possible. Na$^+$ and K$^+$ ions are relatively poor in their solvating capability. DMSO being a solvent of strong donicity [25] can form solvated species with Na$^+$, K$^+$ and, hence, can enhance the IDE. Since PC and DMF are solvents of relatively poor donicity, they do not form stable Na$^+$ and K$^+$ solvated species for intercalation into the graphite lattice.

The threshold potential for intercalation, E_{th}, in all the three solvents is found to have an approximate linear correlation with the overall IDE (Fig. 3(a)). A more positive E_{th} for intercalation naturally means less competition from other reduction processes during intercalation and, hence, higher IDE. This trend was established earlier, even when different graphite substrates were employed [20].

Another interesting correlation is also found to exist between the DPP and IDE (Fig. 3(b)). For TBA$^+$ cations, the DPP does not vary significantly with the solvents. The IDE values are also higher when compared with the IDE values of other cationic species in the same solvent media. For all other cationic species for which intercalation/de-inter-
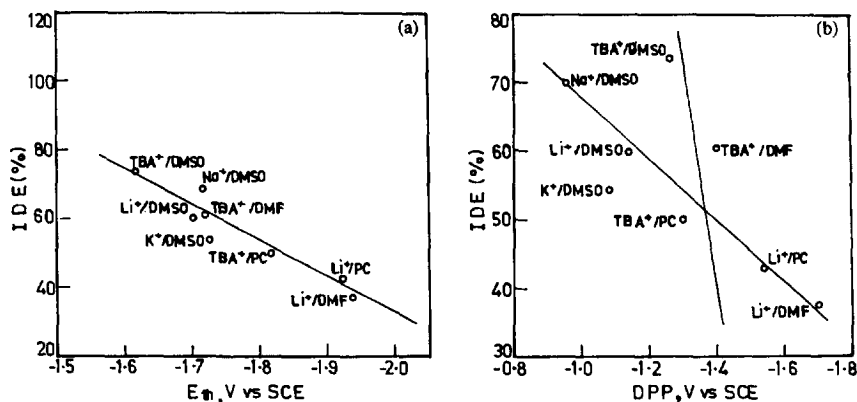

Fig. 3. Cationic intercalation/de-intercalation efficiency vs. (a) threshold potential for intercalation, and (b) de-intercalation peak potential of 0.25 M solution containing corresponding perchlorate salts; scan rate = 40 mV s^{-1}.
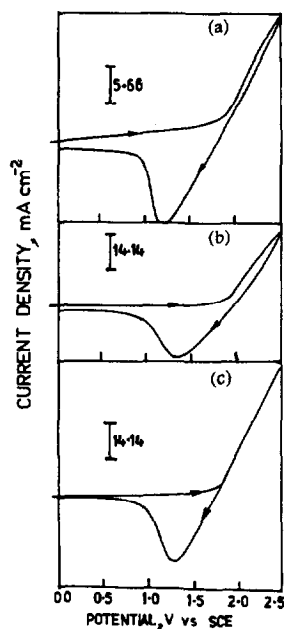
Fig. 4. Cyclic voltammogram for the oxidative intercalation of CPP electrode in (a) PC, (b) AN and (c) MeOH containing 0.25 M LiClO₄; scan rate = 40 mV s⁻¹.
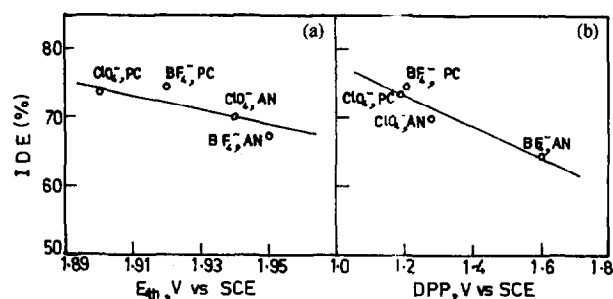

Fig. 5. Anionic intercalation/de-intercalation efficiency vs. (a) threshold potential for intercalation, and (b) de-intercalation peak potential of 0.25 M solution containing ClO₄⁻ ions from LiClO₄ and BF₄⁻ ions from TBAFB.

calation data are available, a linear correlation between IDE and DPP is indeed found. A broad de-intercalation peak covering a wider potential range with more positive DPP naturally leads to higher Q_{di} and hence a higher IDE. Since all the four monovalent cationic species show good intercalation/de-intercalation behaviour in DMSO, further studies were confined to this solvent alone.

3.1.2. Anionic intercalation

Typical cyclic voltammograms for 0.25 M LiClO₄ in different solvents are presented in Fig. 4. Qualitatively, the voltammetric features are quite similar. Quantitative data relating to intercalation/de-intercalation behaviour are summarised in Table 2. The intercalation charge (Q_{in}), as well as the de-intercalation charge (Q_{di}), are generally found to be higher in acetonitrile (AN) media and methanol (MeOH) media. Nevertheless, the overall IDE is found to be better in PC media for ClO₄⁻ anions when LiClO₄ was employed.

The intercalation/de-intercalation behaviour for the same ClO₄⁻ anionic species is found to be quantitatively different when TBAP is employed as the salt in all the three solvents (PC, AN and MeOH). Table 2 clearly shows a poor IDE for TBAP when compared with LiClO₄. The exact cause for this cation dependence of anionic IDE is not clear, although the trend was noticed consistently. It may be due to a higher ionic association between TBA⁺ cations and ClO₄⁻ anions that results in a much lower availability of solvated perchlorate ionic species for intercalation.

There is also a significant difference in the intercalation/de-intercalation behaviour of BF₄⁻ anions among the three solvents, namely, PC, AN and MeOH. The Q_{in} and Q_{di} values are once again higher in AN media, but the overall IDE value is higher in PC (Table 2). Quite interestingly, the BF₄⁻ ion intercalation is extremely low in MeOH medium. The threshold potential for the beginning of intercalation (E_{th}) is close to +1.9 V for a protic solvent such as MeOH. Solvent decomposition, or even decomposition of trace level water (which is inevitably present in this medium) may be the cause of the poor overall efficiency.

Apart from the data obtained from the MeOH medium, the IDE from the other two solvents for both the anionic species is found to exhibit a linear correlation with the E_{th} for intercalation (Fig. 5(a)). There is also a broad linear correlation between IDE and DPP in the case of ClO₄⁻ anions from LiClO₄ and BF₄⁻ anions from TBAFB (tetra-n-butylam-

Table 2

Cyclic voltammetry data for anionic intercalation/de-intercalation processes containing corresponding tetrabutyl ammonium salts on CPP electrode: solvent effects; concentration = 0.25 M; scan rate = 40 mV s⁻¹

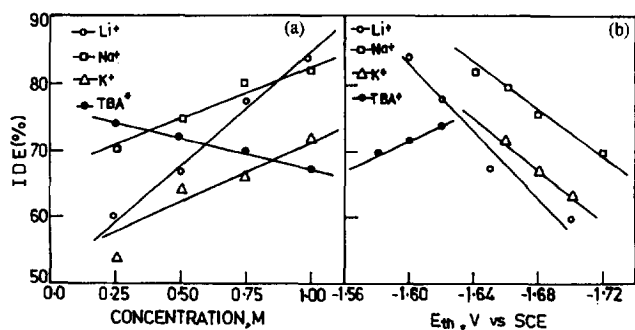| Anion	Solvent	DPP (V)	E_{th} (V)	Q_{in} (mC/cm²)	Q_{di} (mC/cm²)	Q_{di}/Q_{in} (or) IDE
ClO₄⁻ [a]	PC	1.19	1.90	194.43	143.88	0.74
	AN	1.28	1.94	373.70	261.59	0.70
	MeOH	1.25	1.86	856.80	505.51	0.59
ClO₄⁻	PC	1.20	1.70	262.60	91.91	0.35
	AN	1.26	1.80	684.20	212.10	0.31
	MeOH	1.50	1.82	909.00	63.63	0.07
BF₄⁻	PC	1.21	1.92	315.80	236.85	0.75
	AN	1.60	1.95	576.03	391.70	0.68
	MeOH	1.50	1.90	169.80	21.25	0.13

[a] lithium salt.

Fig. 6. Cationic intercalation/de-intercalation efficiency vs. (a) concentration, and (b) threshold potential for intercalation of 0.25 M solution containing corresponding perchlorate salts; scan rate = 40 mV s^{-1}.

monium fluoroborate), as shown in Fig. 5(b). The IDE is generally found to be very low (<0.4) for ClO_4^- anions from TBAP (hence, these data are not shown in Fig. 5). Since PC was found to be an efficient solvent for intercalation of ClO_4^- as well as BF_4^- anions, further investigations on anion intercalation were confined to this medium.

3.2. Effect of electrolyte concentration

3.2.1. Cationic intercalation

Q_{in} and Q_{di} are found to increase systematically with increasing $LiClO_4$ concentration. The IDE, for example, is found to increase from 0.60 to 0.84 when the $LiClO_4$ concentration is increased from 0.25 to 1.0 M (Fig. 6(a)).

In the case of $NaClO_4$, Q_{in} as well as Q_{di} do not increase appreciably beyond the 0.5 M concentration. The overall IDE, however, improves throughout with increase in $NaClO_4$ concentration. The concentration effect on the intercalation of $KClO_4$ is quite similar to that of $NaClO_4$.

A major difference with respect to the concentration effect is noticed for the TBA$^+$ cation. In this case, the cathodic peak currents continue to increase significantly with increasing TBA$^+$ concentration. Nevertheless, the reverse anodic peak current does not increase significantly beyond the 0.5 M TBA$^+$ concentration (Fig. 7). Thus, the overall IDE value is indeed found to decrease slightly with increasing TBAP concentration (Fig. 6(a)). This peculiarity may probably be attributed to the irreversible trapping of TBA$^+$ cations and/ or surface deterioration caused by the large TBA$^+$ cations when higher concentrations are employed. Hence, for TBA$^+$ cations, it appears that lower concentrations provide a higher IDE.

The E_{th} for intercalation varies only very slightly with increasing salt concentration. Despite this, a linear correlation between IDE and E_{th} is found to exist for all these cations, as shown in Fig. 6(b). Again, TBA$^+$ is an exception to the general trend of increasing IDE with more positive E_{th} values. This relationship may be considered as further evidence of the blocking effect of TBA$^+$ cations towards intercalation with increasing concentration.
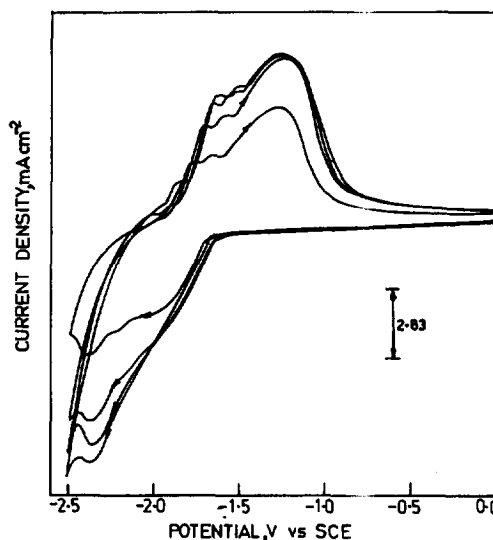

Fig. 7. Cyclic voltammogram for the reductive intercalation of CPP electrode in different concentrations of TBAP–DMSO solutions. Concentration (M): (a) 0.25; (b) 0.50; (c) 0.75, and (d) 1.0; scan rate = 40 mV s^{-1}.

3.2.2. Anionic intercalation

The general trend of increasing Q_{in} as well as IDE with increasing concentration for anions is noticed for $LiClO_4$, TBAP and TBAFB. In the case of TBAP, the solubility constraints limit the maximum concentration to 0.65 M. Among the three salts employed under identical conditions, the IDE is found to decrease in the order TBAFB > $LiClO_4$ > TBAP.

In the case of TBA$^+$ cationic intercalation, IDE was in fact found to decrease slightly with increasing concentration (Figs. 6(a) and 7). In the case of anions, however, the IDE increases consistently with concentration (Fig. 8(a)). Strong adsorption effects noted in the case of TBA$^+$ cations are not prevalent for anionic intercalation. Hence, anionic intercalation displays a significant concentration dependence. A linear relationship is again found between E_{th} and IDE for ClO_4^- anions from $LiClO_4$ and BF_4^- anions from TBAFB with varying concentrations (Fig. 8(b)). The data also indicate that the IDE increases substantially with concentration for BF_4^- anions when compared with ClO_4^- anions.

3.3. Effect of sweep rate

The irreversibility in the intercalation/de-intercalation processes may generally be associated with slow surface transformations and trapping processes. At shorter time scales or higher sweep rates, a higher overall IDE would be expected. This is indeed found to be the case for all the cationic species investigated in DMSO medium. For example, the IDE for Li$^+$ intercalation increases from 0.84 at 40 mV s^{-1} to 0.94 at 320 mV s^{-1}.

The sweep rate also has the same type of influence for anionic intercalation in PC medium. For example, the IDE for ClO_4^- intercalation increases from 0.79 at 40 mV s^{-1} to 0.88 at 320 mV s^{-1}.
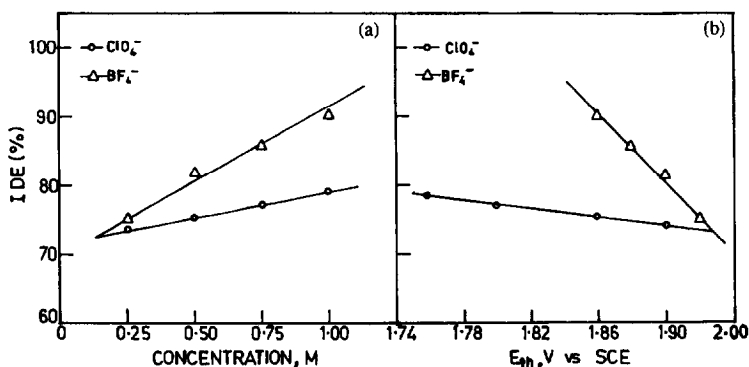
Fig. 8. Anionic intercalation/de-intercalation efficiency vs. (a) concentration, and (b) threshold potential for intercalation of 0.25 M solution containing ClO_4^- ions from $LiClO_4$ and BF_4^- ions from TBAFB; scan rate = 40 mV s⁻¹.

3.4. Effect of potential cycling

Under optimum conditions, the intercalation/de-intercalation processes are generally found to be quite reversible. This aspect has also been confirmed by earlier workers [4,9]. Multi-sweep cyclic voltammetric curves were found to retrace one another very closely. A typical cyclic voltammogram for cationic intercalation in 1.0 M $LiClO_4^-$–DMSO solutions is presented in Fig. 9. A very similar trend was observed in the case of other cationic intercalation from DMSO medium. Reproducible cyclic voltammetric responses were also obtained for both ClO_4^- and BF_4^- anionic species. In general, the experiments suggest the possibility of using these intercalation/de-intercalation processes for rechargeable battery development.

3.5. Effect of cathodic potential limit

With increasing cathodic potential limit, Q_{in} as well as Q_{di} are found to increase. Quite interestingly, the IDE for all the cationic species are maximum when the cathodic limit is set at −2.5 V. This interesting observation is brought out clearly in Fig. 10(a). It seems that the competitive reduction process
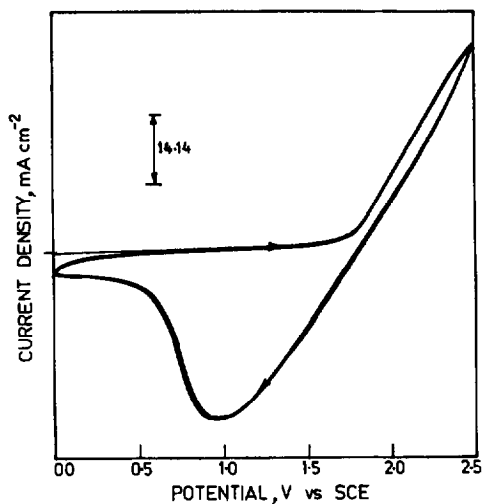
becomes more predominent in presence of all these electrolyte systems beyond −2.5 V. In DMSO, the competitive process appears to be independent of the nature of the supporting electrolyte. The competitive process should probably be solvent decomposition itself.

The multiple peaks observed in the cyclic voltammograms whenever TBA⁺ cations are involved probably correspond to different stages of intercalation. These steps, however, may also be attributed to different surface states of graphite plates in the polypropylene matrix.

The anodic potential limit is also found to have quite similar influence on the IDE of ClO_4^- anions from $LiClO_4$ as well as BF_4^- anions from TBAFB. The IDE continues to increase up to +2.5 V for both these ionic species (Fig. 10(b)). Beyond this potential limit, the effect of competitive anodic processes become significant and hence IDE decreases with further increase in anodic potential limit.

Fig. 9. Multi-sweep cyclic voltammogram for the oxidative intercalation of CPP electrode in 1.0 M $LiClO_4$–PC solutions (5 cycles); scan rate = 40 mV s⁻¹.
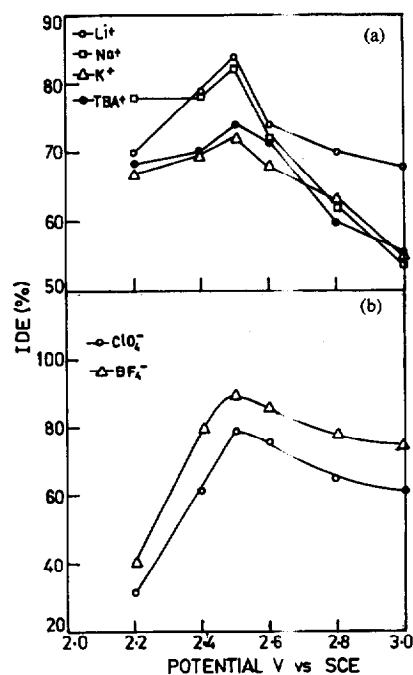

Fig. 10. Cationic intercalation and de-intercalation efficiency vs. potential limit for (a) cations in 1.0 M DMSO solutions, and (b) anions in 1.0 M PC solutions; scan rate = 40 mV s⁻¹.

3.6. X-ray diffraction measurements

The intercalated graphite samples were prepared by polarizing the CPP graphite material at the intercalation potential (−2.5 V for cations, +2.5 V for anions) for 5 h. The collected powdery material was subjected to XRD analysis.

XRD measurements confirm the formation of distinct intercalated crystalline phases. Non-intercalated graphite samples gave the characteristic d value of the graphite lattice, viz., 3.34 Å. The intercalated samples showed some additonal d values corresponding to the compressed diameter of solvated or desolvated cationic species. The data for all the cationic and anionic systems are summarized in Table 3. Similar d values for cationic intercalation in non-aqueous solvents have been reported by earlier workers [7,26].

3.7. Thermogravimetric and differential thermal analysis

The thermal properties of cation-intercalated graphite samples were also evaluated using thermogravimetric (TG) and differential thermal analysis (DTA). Typical data for Li^+ and TBA^+ intercalated graphite samples are presented in Fig. 11(a) and (b), respectively. In all the four cases (Li^+, Na^+, K^+ and TBA^+), the TG graphs show distinct weight loss regions over the temperature range of 30 to 500 °C. DTA indicates some endothermic processes below 150 °C for all the cations. Similar endothermic DTA peaks have been attributed [13] to solvent evaporation from the surface of the intercalated samples. It is significant to note that this endothermic peak is minimum for TBA^+ cation (Fig. 11(b)). In all other cases, an endothermic solvent evaporation process plays a much more significant role. This confirms the earlier assumption (Section 3.1.) that the TBA^+ cations undergo intercalation without solvation.

Thermal processes beyond 150 °C are generally exothermic in nature. In the case of Li^+ and TBA^+, a sharp exothermic peak is observed around 200 °C (Fig. 11). In the case of Na^+ and K^+ ions, the exothermic peak occurs around 350 °C. Even among these two cationic species, the DTA peak for K^+ ions is much sharper than that for Na^+ ions. These exothermic processes are associated with the solvent evaporation from the interior of the graphite lattice.

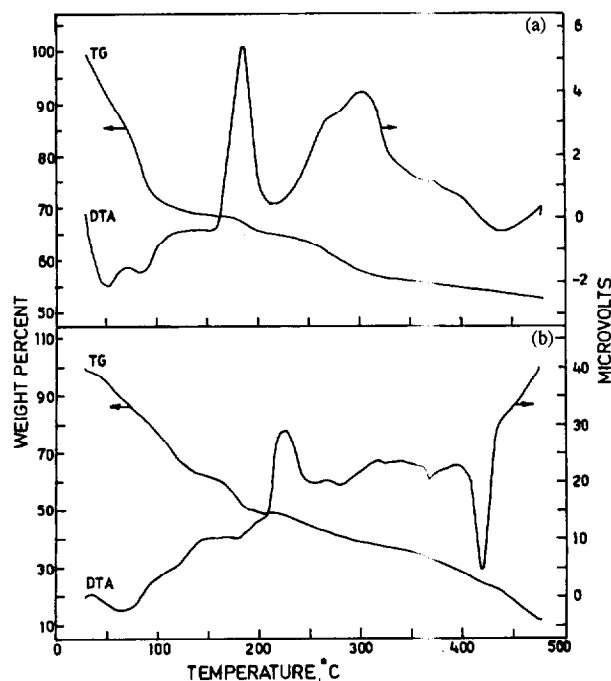In the DTA graph corresponding to TBA^+ cation (Fig. 11(b)), a distinct endothermic peak is noticed around 420

Fig. 11. TG and DTA curves of the CPP electrode electrolysed cathodically at a potential of −2.5 V for 5 h. Speed of rise in temperature: 5 °C min⁻¹. (a) 1.0 M LiClO₄–DMSO solution, and (b) 0.25 M TBAP–DMSO solution.

°C. The exact cause for this endothermic process is not clear. The overall thermal properties of all the four cation-intercalated graphite samples are quite similar to those reported earlier in the literature [12,13].

The anion-intercalated graphite samples were also subjected to TG and DTA. Both intercalated samples show endothermic processes at low temperatures and exothermic processes at higher temperatures. In this respect the TG/DTA data are quite similar to those obtained for cation-intercalated systems. The DTA curve at higher temperatures for the anion-intercalated sample does not exhibit any sharp exothermic peaks.

4. Conclusions

The present investigation highlights the important role of solvent in cationic, as well as anionic, intercalation/de-intercalation processes. A solvent of high donor number, such as DMSO, behaves as a good solvent for all the monovalent cations investigated. A solvent of high acceptor number, such as PC, is indeed the solvent of choice for ClO_4^- as well as BF_4^- anion-intercalation in terms of IDE. Acetonitrile, however, gives a slightly higher intercalation and de-intercalation charges. Li^+ cations, that can interact very strongly with any solvent, also serve as a good solvated intercalation species. Cations with good hydrophobicity, such as TBA^+ cations, can also undergo intercalation without a solvation sheath and hence intercalate efficiently in all solvents. The IDE increases with increasing concentration for all the monovalent cations, as well as anions, except the TBA^+ cation. Irreversible trap-

Table 3
XRD data (d, 2θ) for different ionic species intercalated CPP graphite material. concentration: 1.0 M; intercalation potential: −2.5 V; intercalation time: 5 h

Solvent	Ion	d value (Å)	2θ
DMSO	Li^+	4.13	21.5
	Na^+	3.57, 5.18	24.9, 17.1
	K^+	5.21	17.0
	TBA^+	3.66, 7.13	24.3, 12.4
PC	ClO_4^-	5.27	16.8
	BF_4^-	5.21	17.0

ping, leading to poor overall IDE, is a slow process and occurs predominantly only at slower sweep rates. The IDE for anion intercalation is significantly higher when $LiClO_4$ is used instead of TBAP. BF_4^- ion intercalation is significantly more efficient. The optimum intercalation potential for all the cations and anions is found to be -2.5 and $+2.5$ V, respectively. The same CPP electrode could be cycled for a number of times. The presence of an intercalated phase is confirmed by XRD measurements for all the ionic species. TG and DTA also confirm two stages of solvent removal, the first is an endothermic one (involving desolvation from the surface) while the second is an exothermic one (involving desolvation from the interior of the electrode).

Acknowledgements

References

[1] J.O. Besenhard and H.P. Fritz, J. Electroanal. Chem., 53 (1974) 329.
[2] J.O. Besenhard, Carbon, 14 (1976) 111.
[3] J. Simonet and H. Lund, J. Electroanal. Chem., 75 (1977) 719.
[4] Y. Maeda and S. Harada, Synth. Met., 31 (1989) 389.
[5] Y. Maeda, J. Electrochem. Soc., 137 (1990) 3047.
[6] Y. Maeda, D. Sugimori and M. Inagaki, Tanso, (1991) 244.
[7] D. Billand, F.X. Henry and P. Willmann, Mater. Res. Bull., 28 (1993) 477.
[8] Z.X. Shu, R.S. Mc Millan and J.J. Murray, J. Electrochem. Soc., 140 (1993) 922.
[9] D. Aurbach, Y. Ein-Eli, O. Chusid, Y Carmeli, M. Babai and H. Yamin, J. Electrochem. Soc., 14 (1994) 603.
[10] R. Yazami, K. Zaghib and M. Deschamps, J. Power Sources, 52 (1994) 55.
[11] T. Tran and K. Kinoshita, J. Electroanal Chem., 386 (1995) 221.
[12] Y. Maeda, Ph. Touzain and L. Bonnetain, Synth. Met., 24 (1988) 267.
[13] Y. Maeda and Ph. Touzain, Electrochim Acta, 33 (1988) 1493.
[14] T. Ohzuku, Z. Takehara and S. Yoshizawa, Denki Kagaku, 46 (1978) 438.
[15] Y. Matsuda, M. Morita and H. Katsuma, Denki Kagaku, 51 (1983) 744.
[16] R. Santhanam and M. Noel, J. Power Sources, 56 (1995) 101.
[17] F. Beck, H. Junge and H. Krohn, Electrochim Acta., 26 (1981) 799.
[18] F. Beck, H. Krohn and W. Kaiser, J. Appl. Electrochem., 12 (1982) 505.
[19] F. Beck and H. Krohn, Synth. Met., 14 (1986) 137.
[20] R. Santhanam and M. Noel, J. Power Sources, 63 (1996) 1.
[21] J.N. Butler, J. Electroanal. Chem., 14 (1967) 89.
[22] D.T. Swayer and J.C. Roberts, Experimental Electrochemistry for Chemists, Wiley, 1974, p. 209.
[23] T. Ohzuku, Z. Takehara and S. Yoshizawa, Denki Kagaku, 46 (1978) 438.
[24] R. Santhanam, Ph.D. Thesis, Madurai Kamaraj University, Madurai, India, 1996.
[25] V. Gutmann, Electrochim. Acta, 2 (1976) 661.
[26] M.F. Quinton, A.P. Legrand and F. Beguin, Synth. Met., 14 (1986) 179.